chemosensors

MDPI

Review

Bicyclic 1,3a,6a-Triazapentalene Chromophores: Synthesis, Spectroscopy and Their Use as Fluorescent Sensors and Probes

Yingchun Wang, Tomas Opsomer and Wim Dehaen *

Molecular Design and Synthesis, Department of Chemistry, KU Leuven, Celestijnenlaan 200F, 3001 Heverlee, Belgium
* Correspondence: wim.dehaen@kuleuven.be

Abstract: The 1,3a,6a-triazapentalene (TAP) is an aromatic heterocyclic fluorescent dye with interesting features such as its small size, large Stokes shift, solvatochromism, and emission wavelengths that are spread across the visible spectrum. TAPs have been synthesized via different synthetic strategies involving click−cyclization−aromatization domino reactions, gold-catalyzed cyclization of propargyl triazoles or triazolization of acetophenones. As a result, TAPs with diverse substitution patterns were obtained, showing varying fluorescence properties. Based on these properties, several TAPs have been selected and studied as fluorescent imaging probes in living cells and as sensors. This mini review provides an overview of the research on the bicyclic TAPs and does not comment on the literature about benzo or otherwise fused systems. The synthetic methodologies for the preparation of TAPs, the substituent effects on the fluorescence properties, and the behavior of the TAP core as an element of biological imaging probes and sensors are discussed.

Keywords: 1,3a,6a-triazapentalene; synthetic methods; fluorescence properties; fluorescent imaging probes; fluorescent sensors; living cells

Citation: Wang, Y.; Opsomer, T.; Dehaen, W. Bicyclic 1,3a,6a-Triazapentalene Chromophores: Synthesis, Spectroscopy and Their Use as Fluorescent Sensors and Probes. *Chemosensors* **2021**, *9*, 16. https://doi.org/10.3390/chemosensors9010016

Received: 17 December 2020
Accepted: 12 January 2021
Published: 15 January 2021

1. Introduction

Organic fluorophores have been widely applied in modern science and technology as biological labels and probes [1–6], fluorescent sensors [7–11], etc. Advances in these applications are often driven by the development of new fluorescent dyes, aiming to acquire the desired physicochemical and photophysical properties. Therefore, the design of novel organic dyes and studying synthetic pathways for their preparation are relevant research areas that have received ample attention in recent decades [12–16]. However, most organic fluorophores are relatively large and hydrophobic, limiting their use in aqueous systems. In this regard, the 1,3a,6a-triazapentalene (TAP) sparked considerable interest upon its introduction a decade ago as a novel 10π-electron fluorophore due to its small size [17,18]. Generally, 1,3a,6a-triazapentalenes can be categorized into two types: (1) (hetero)aryl-fused and (2) the non-fused, simply bicyclic parent TAPs (Figure 1).

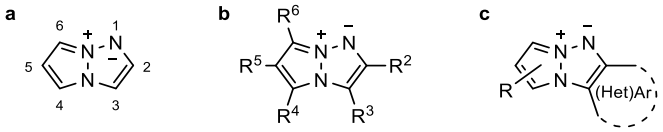

Figure 1. Numbering of the 1,3a,6a-triazapentalene (TAP) core (**a**) and the general structures of non-fused TAPs (**b**) and (hetero)aryl-fused TAPs (**c**).

The (hetero)aryl-fused TAPs were reported for the first time in 1965 [19], and published methods to synthesize fused TAPs involve the deoxygenation of 1-(*o*-nitro(hetero)aryl)pyrazoles and thermolysis or photolysis of 1-(*o*-azido(hetero)aryl)pyrazoles [18–22], among others [23,24]. In general, the fluorescence properties of these fused TAPs are much less described, and this is

why we will not include them in this literature study. However, we should mention a recent (2020) synthetic method based on intramolecular *N*-*N* bond formation of pyrazole-substituted aminopyridines and aminodiazines in the presence of hypervalent iodine(III) leading to tricyclic TAP derivatives with fluorescent behavior, that was published by Suzenet et al. [25]. This is a very interesting new development in TAP chemistry.

The bicyclic TAPs, which are the subject of this mini review, have been prepared via different synthetic pathways. Hirobe et al. were the first to report the bicyclic (non-fused) triazapentalenes in 1978 [26]. However, during the decades that followed, this heterocyclic scaffold was somehow not further studied, until a reappearance was made in 2011 [17]. Namba et al. cleverly applied the copper-catalyzed azide-alkyne cycloaddition (CuAAC) reaction for the synthesis of the parent TAPs, which resulted in a number of valuable studies published by this group throughout the past decade [27–30]. Furthermore, these findings also encouraged other researchers to study the TAP fluorophore and to develop alternative methods for their preparation [31,32].

In this mini review, we will cover the different synthetic methods toward bicyclic triazapentalenes, along with the photophysical data and applications of the respective dyes. Throughout the remaining part of this text, TAP will only refer to bicyclic, non-aryl-fused triazapentalenes.

2. Synthetic Methods and Spectroscopic Properties

2.1. Aminopyrazole-Mediated Syntheses

The bicyclic 1,3a,6a-triazapentalenes, firstly reported by the Hirobe group, were synthesized via two different reaction pathways (Scheme 1) [26]. One pathway involved the synthesis of 3-acetyl-2-methyl-TAP **4**. Starting from the parent pyrazole **1** and hydroxylamine-*O*-sulfonic acid **2**, 1-aminopyrazole **3** was prepared and further reacted with 3-chloropentane-2,4-dione at elevated temperatures. In the next step, the resulting TAP **4** could be deacetylated under acidic conditions to afford the colorless 2-methyl-TAP **5** in the 95% yield. In another pathway, the 2-phenyl-TAP derivative **8** was synthesized through the amination of phenacylpyrazole **7** with *O*-(mesitylenesulfonyl)hydroxylamine **6**. Interestingly, the deacetylated TAP **5** appeared to be sensitive to air and distinctly less stable compared to the 3-acyl derivative **4**. The 2-phenyl-TAP **8** was slightly more stable than its methyl analog **5**. From this initial study, the authors already recognized the stabilizing effect of an electron withdrawing group on the TAP core.

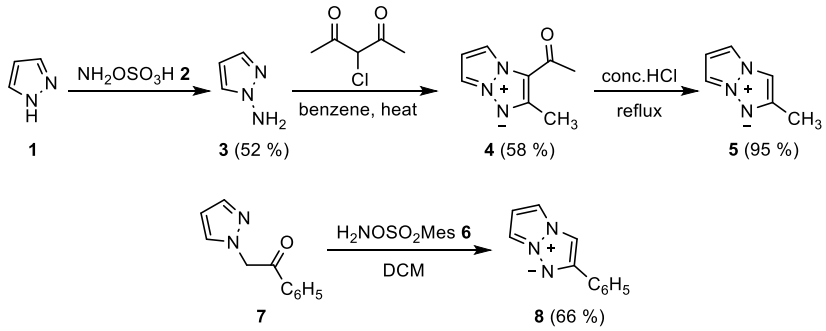

Scheme 1. Synthesis of 2-methyl-TAP **5** and 2-phenyl-TAP **8**.

2.2. CuAAC-Based Syntheses

Namba et al. envisioned the renowned copper-click reaction as a valuable tool for the preparation of TAPs [17]. Starting from terminal alkynes **9** and 1-azidopropane building blocks **10** containing leaving groups (LG) at positions 2 and 3, the azide-alkyne cycloaddition in the presence of catalytic Cu(I) provided 1,2,3-triazoles as intermediate substrates. Next, cyclization of the 1,2,3-triazoles easily occurred in the basic environment via the substitution of one leaving group and was followed by the elimination of the second leaving group, causing aromatization (Scheme 2). Normally, the substituents on the azidopropanes

were trifluoromethanesulfonate (triflate) groups. By changing the substituents on the alkynes and introducing additional side groups on the azido substrates, 3-unsubstituted TAP derivatives with various functionalization patterns were obtained by means of this general reaction pathway.

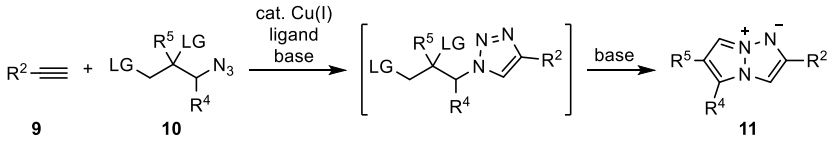

Scheme 2. CuAAC-based synthesis of 3-unsubstituted TAPs **11**.

2.2.1. The 2-Substituted 1,3a,6a-Triazapentalenes

Various 2-substituted TAPs **12** were synthesized by the Namba group starting from terminal alkynes **9** and 3-azido-propane-1,2-diyl bistriflate **10a** (Scheme 3) [17,28]. The reactions were carried out with copper(I) iodide, bis[2–(*N*,*N*-dimethylamino)ethyl] ether (BDMAEE) ligand and triethylamine (TEA) base in tetrahydrofuran (THF). It was found that the presence of an electron withdrawing group at the C2 position led to better reaction yields. Whereas the reaction with 4-nitrophenylacetylene reached a 96% yield of TAP **12g**, TAP **12d** with a 4-methoxyphenyl substituent was only obtained with a yield of 56%. Intriguingly, the unsubstituted triazapentalene **12b** was obtained for the first time by the direct desilylation of crude 2-trimethylsilyl-TAP **12a**. However, TAPs lacking an aryl substituent and 4-methoxyphenyl-TAP **12d** gradually decomposed under UV irradiation. Therefore, it was confirmed that an electron poor aryl group is needed to stabilize the TAP core.

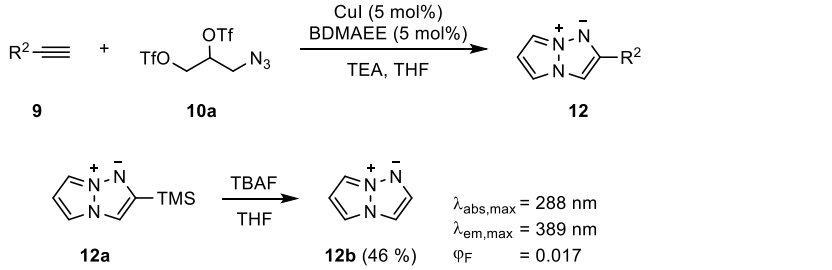

Scheme 3. The synthesis of 2-substituted TAPs **12** and the parent TAP **12b**.

The fluorescent properties of TAPs were investigated by Namba et al. already in this first report and in subsequent articles. As indicated in Table 1, it was clear that the emission maxima of 2-substituted TAP in dichloromethane (DCM) underwent a bathochromic shift as the Hammett σ_p value of the para substituted phenyl groups increased from −0.28 to 0.81 (Table 1) [17,28]. As a result of introducing additional electron withdrawing groups on the aryl group, compounds **12i** and **12j** exhibited bathochromically shifted yellow and red fluorescence, respectively [28]. Moreover, the Stokes shifts of these 2-substituted TAPs were between 83 and 166 nm, which are rather large values. Notably, compounds **12f** and **12i** showed a strong positive solvatochromism as the emission maxima increased with 72 nm and 99 nm, respectively, when changing the solvent from benzene to acetone. The trends based on the Hammett values and the solvatochromic effect might be of use to predict the emission wavelengths of TAPs with other substituents at position 2 and in different solvents. Unfortunately, the quantum yields of the fluorescence of most 2-substituted TAPs were rather low (3–44%).

Table 1. Fluorescence properties and reaction yields of selected 2-substituted TAPs **12c–g** in DCM.

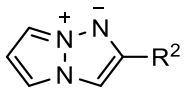	**R²**							
							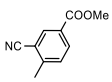	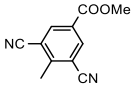
Compound	**12c**	**12d**	**12e**	**12f**	**12g**	**12h**	**12i**	**12j**
Yield (%)	89	56	81	70	96	73	71	72
$\lambda_{abs,max}$ (nm)	326	330	345	381	412	376	420	466
Hammett σ_p	0	−0.28	0.04	0.71	0.81	-[a]	-[a]	-[a]
$\lambda_{em,max}$ (nm)	419	413	456	509	556	510	572	632
Stokes shift (nm)	93	83	111	128	144	134	152	166
φ_F (%)	3	6	24	18	16	44	34	10

[a] No data available.

2.2.2. The 2,5-Disubstituted 1,3a,6a-Triazapentalenes

The 2,5-disubstituted 1,3a,6a-triazapentalenes were prepared via the general procedure by using 2-substituted 3-azido-2-methoxypropyl triflates **10b** [27]. In this case, the aromatization failed when using triethylamine as the base. In addition, in the presence of DBU as a stronger base or in an acidic environment, elimination of the methoxy group did not happen. However, the elimination occurred by using KHMDS at −78 °C, and 2,5-disubstituted TAPs **13** were obtained successfully (Scheme 4) [27]. Nearly all reaction yields were good, except for the examples with a phenyl group at the C5 position (**13d**) or with a 4-nitrophenyl substituent at position 2 (**13i**). Note that the latter derivatives were prepared without heating to reflux temperature or by using lithium diethylamide base, respectively.

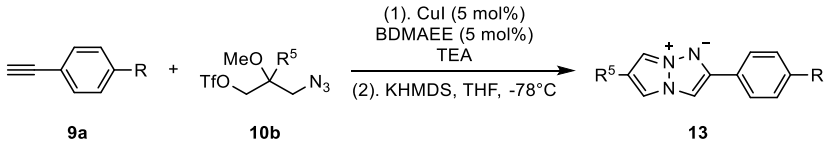

Scheme 4. Synthesis of 2,5-disubstituted TAPs **13**.

An interesting observation was that the quantum yields of fluorescence for **13ad** were dramatically increased as a result of introducing a functional group at the C5 position of 2-cyanophenyl-TAP **12f**, as shown in Table 2 [27]. Moreover, these functional groups at the C5 position had no obvious effect on the emission wavelengths, except for the introduction of a 5-cyano group that caused a hypsochromic effect on both the absorption and emission wavelengths. When changing the aryl substituent at the C2 position of different 5-methyl-TAPs, the quantum yields substantially increased when the Hammett values σ_p increased from 0 to 0.71, as shown in Table 3. For the 4-methoxyphenyl (σ_p = −0.28) and the 4-nitrophenyl (σ_p = 0.81) substituents, the quantum yields were only 0.02 and 0.03, respectively. Thus, for some examples, a relation could be noticed between the quantum yield of 2-arylated 5-methyl-TAPs and the Hammett parameter of the phenyl substituent.

Table 2. Fluorescence properties and reaction yields of 5-substituted 2-cyanophenyl-TAPs **13a–d** in DCM.

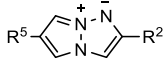	**R⁵**				
	Me	**OMe**	**-CN**	**Ph**	**H**
$R^2 = C_6H_4CN$	**13a**	**13b**	**13c**	**13d**	**12f**
Yield (%)	63	60	57	19	70
$\lambda_{abs,max}$ (nm)	385	378	360	383	381
$\lambda_{em,max}$ (nm)	518	505	453	506	509
Stokes shift (nm)	133	127	93	123	128
φ_F (%)	55	57	45	48	18

Table 3. Fluorescence properties and reaction yields of 2-substituted 5-methyl-TAPs **13e–i** in DCM.

	R^2				
R^5 = CH_3	**13e**	**13f**	**13g**	**13h**	**13i**
Yield (%)	81	72	59	63	27
$\lambda_{abs,max}$ (nm)	340	340	370	385	370
Hammett σ_p	0	−0.28	0.04	0.71	0.81
$\lambda_{em,max}$ (nm)	422 (419) [a]	421 (413) [a]	466 (456) [a]	518 (509) [a]	575 (556) [a]
Stokes shift (nm)	82	81	96	133	205
φ_F (%)	7 (3) [b]	3 (6) [b]	27 (24) [b]	55 (18) [b]	2 (16) [b]

[a] Fluorescence maximum of corresponding 5-unsubstituted analog. [b] Fluorescence quantum yield of corresponding 5-unsubstituted analog.

2.2.3. The 2,4-Disubstituted 1,3a,6a-triazapentalenes

To investigate the effect of substituents at the C4 position, various 4-methyl and 4-phenyl-TAP analogs were synthesized by the Namba group (Scheme 5) [29]. The yields of the 4-methyl-TAP analogs were more variable (19–94%) (Table 4). On the other hand, the 4-phenyl-TAPs were obtained in moderate-to-high yields (50–88%) (Table 5). For some derivatives, the low yields were attributed to decomposition during purification. To expand the scope of 4-methyl-TAP analogs, 1,4-diethynylbenzene **9b** and cyclic strained alkyne **9c** were applied to synthesize **14a** and **14b**, respectively, via the reaction with 3-azido-3-methylpropane-1,2-diyl bistriflate. The designed compound **14a** was not obtained as the reaction stopped after the mono-TAP was formed. This intermediate was readily decomposed during purification. Compound **14b** was obtained successfully in 49% yield via the general procedure but without the use of a copper catalyst. For comparison, similar reactions were carried out to afford the corresponding 4-unsubstituted TAPs **12k** and **12l** in 46% and 51% yields, respectively.

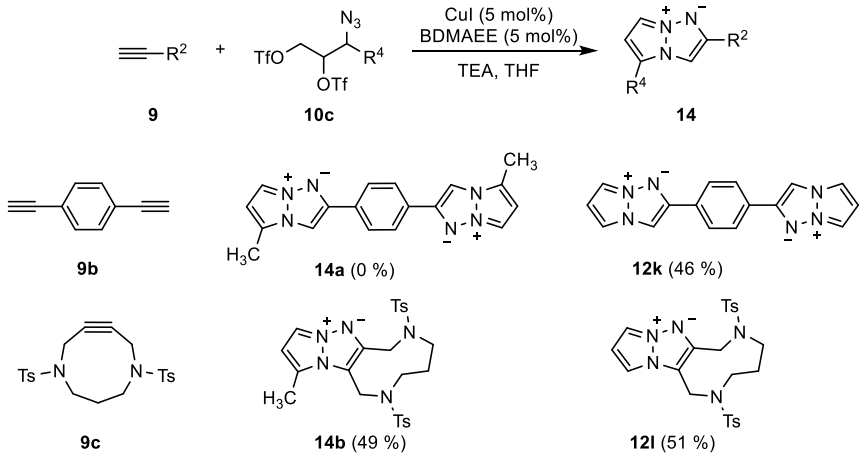

Scheme 5. The synthesis of 2,4-disubstituted TAPs **14** and corresponding 4-unsubstituted TAPs. R^4 = Me or Ph.

Table 4. Fluorescence properties and reaction yields of 2-substituted 4-methyl-TAPs **14c–h** in DCM.

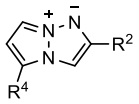	**R²**					
	-COOMe	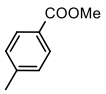	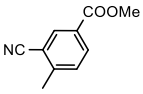			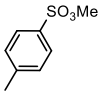
$R^4 = CH_3$	**14c**	**14d**	**14e**	**14f**	**14g**	**14h**
Yield (%)	94 (90) [a]	82 (73) [a]	19 (71) [a]	60 (74) [a]	28 (81) [a]	50(40) [a]
$\lambda_{abs,max}$ (nm)	354 (342) [b]	380 (376) [b]	436 (420) [b]	356 (358) [b]	360 (345) [b]	393 (379) [b]
$\lambda_{em,max}$ (nm)	456 (431) [c]	553 (521) [c]	611 (572) [c]	485 (460) [c]	491 (456) [c]	558 (525) [c]
Stokes shift (nm)	105	173	175	129	131	165
φ_F (%)	24 (18) [d]	56 (44) [d]	11 (34) [d]	8 (35) [d]	40 (24) [d]	40 (43) [d]

[a] Reaction yield of 4-unsubstituted analog. [b] Absorption maximum of corresponding 4-unsubstituted analog. [c] Fluorescence maximum of corresponding 4-unsubstituted analog. [d] Quantum yield of corresponding 4-unsubstituted analog.

Interestingly, the emission maxima of 4-phenyl-TAP (such as **14m**, $\lambda_{em,max}$ = 613 nm) and 4-methyl-TAP (such as **14e**, $\lambda_{em,max}$ = 611 nm) analogs were similar to each other [29]. Therefore, it could be concluded that the expansion of π–conjugation between the C4 phenyl and TAP core did not show an effect on the emission wavelength. To compare with 4-unsubstituted TAPs, the extinction coefficient (ε) values of 4-phenyl analogs were measured at slightly longer absorption wavelengths and larger ε values were observed, which may enhance the brightness as for **14j** and **14k** (Table 5). Remarkably, both a methyl and phenyl group at the C4 position could induce a redshift of the maximum emission wavelength.

Table 5. Fluorescence properties and reaction yields of 2-substituted 4-phenyl-TAPs **14i–o** in DCM.

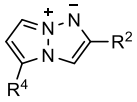	**R²**						
	-COOMe		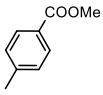		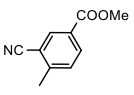		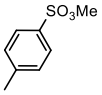
R^4 = Ph	**14i**	**14j**	**14k**	**14l**	**14m**	**14n**	**14o**
Yield (%)	87	70	82	81	88	72	50
$\lambda_{abs,max}$ (nm)	358 (342) [a]	387 (381) [a]	383 (376) [a]	342 (358) [a]	432 (420) [a]	369 (345) [a]	378 (358) [a]
$\lambda_{em,max}$ (nm)	459 (431) [b]	542 (509) [b]	548 (521) [b]	481 (460) [b]	613 (572) [b]	482 (456) [b]	554 (525) [b]
Stokes shift (nm)	101	155	165	139	181	113	176
φ_F (%)	9 (18) [c]	46 (15) [c]	36 (44) [c]	8 (35) [c]	7 (34) [c]	10 (20) [c]	21 (43) [c]
ε (dm^3 mol^{-1} cm^{-1})	10,648 (2691) [d]	6918 (3032) [d]	7500 (1230) [d]	19,822 (4213) [d]	4560 (631) [d]	19,409 (5011) [d]	5497 (2542) [d]

[a] Absorption maximum of corresponding 4-unsubstituted analog. [b] Fluorescence maximum of corresponding 4-unsubstituted analog. [c] Quantum yield of corresponding 4-unsubstituted analog. [d] Extinction coefficient value of corresponding 4-unsubstituted analog.

2.2.4. The 2,6-Disubstituted 1,3a,6a-Triazapentalenes

To obtain the 2,6-disubstituted TAPs, the initial plan was to use the general procedure starting from 3-azido-1-methylpropane-1,2-diyl bistriflates and terminal alkynes. However, the methylazidoditriflate was not stable enough to prepare. In 2013, Namba et al. reported a Payne-type rearrangement of 1-(oxiranylmethyl)-1,2,3-triazoles [33]. Based on this earlier study, a reported procedure was developed for the synthesis of 2,6-disubstituted 1,3a,6a-triazapentalenes **21**. The intermediate **20** was formed by the triflic acid-mediated epoxide-opening reaction, then followed by the subsequent reactions of acetylation and base-induced elimination (Scheme 6) [30]. Due to the poor stability of the 6-methyl-substituted TAPs, all reaction yields were relatively low (Table 6), while the more stable 6-(methoxycarbonyl)-TAP **23** was obtained in 40% yield. On the other hand, the 6-phenyl-TAP was not obtained after attempts under various conditions.

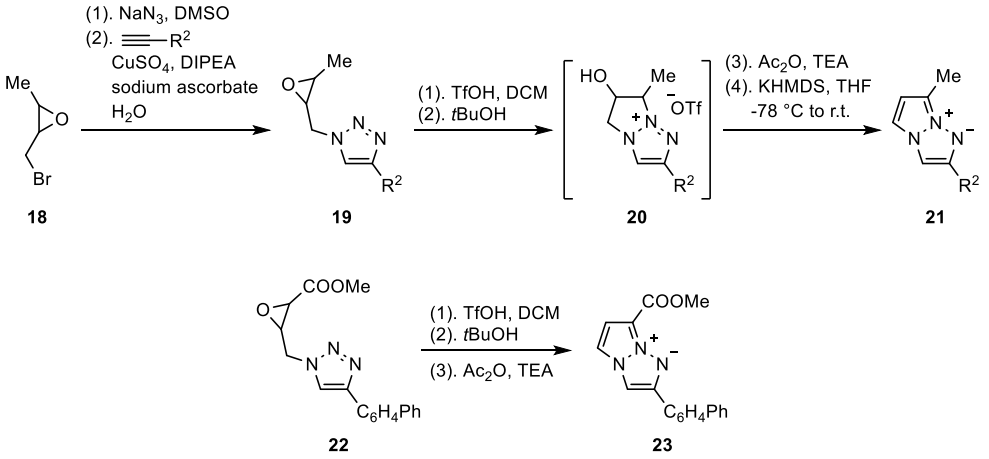

Scheme 6. Synthesis of 2,6-disubstituted TAPs **21** and **23**.

Introducing the methyl group at the C6 position of 2-substituted 1,3a,6a-triazapentalenes not only induced a long-wavelength shift of the emission maxima but also affected the quantum yields (Table 6) [30]. Nearly all the quantum yields were somewhat increased, except for compounds **21d** and **21e**. Notably, the methoxycarbonyl group at the C6 position (**23**) quenched the fluorescence. It was assumed that the electron withdrawing group disturbed the charge transfer between the TAP core and C2 substituents.

Table 6. Fluorescence properties and reaction yields of selected 2-substituted 6-methyl-TAPs **21a–e** in DCM.

	R^2				
R^6	CN		Ph	COPh	$-C_{13}H_{27}$
$R^6 = CH_3$	**21a**	**21b**	**21c**	**21d**	**21e**
Yield (%)	24	26	37	18	14
$\lambda_{abs,max}$ (nm)	390 (381) [a]	341 (326) [a]	362 (345) [a]	400 (390) [a]	357 (334) [a]
$\lambda_{em,max}$ (nm)	545 (509) [b]	435 (419) [b]	493 (456) [b]	654 (608) [b]	487 (482) [b]
Stokes shift (nm)	155	94	131	254	130
φ_F (%)	26 (15) [c]	17 (3) [c]	24 (20) [c]	2 (20) [c]	1 (4) [c]

[a] Absorption maximum of the corresponding 6-unsubstituted analog. [b] Fluorescence maximum of the corresponding 6-unsubstituted analog. [c] Quantum yield of corresponding to the 6-unsubstituted analog.

2.3. Gold-Catalyzed Cyclization of Propargyl-1,2,3-Triazoles

In 2010, Shi et al. reported an efficient method to synthesize propargyl-1,2,3-triazoles **24** via the iron-catalyzed alkylation with propargyl alcohols and found that the N2-substituted propargyl triazoles **24** could be further transformed via the intramolecular gold-catalyzed triazole-yne cyclization (Scheme 7) [34]. Later in 2014, the same group demonstrated that this cyclization resulted in the formation of TAPs **27** by using propargyl triazoles **24** bearing an electron withdrawing group (Scheme 7) [31]. The electron withdrawing group on the triazole ring, mainly ketones and esters, changed the electron density distribution of the intermediate bicyclic system. This electron density redistribution induced an effective regioselection followed by protodeauration to afford differently substituted triazapentalenes **27**. In general, ester-substituted TAPs were obtained in slightly lower yields. However, the diester-substituted TAPs were shown to form in high yields (over 80%). Furthermore, starting from mono ester-substituted TAPs, 3-unsubstituted TAPs were obtained via LiOH-induced saponification/decarboxylation.

As mentioned by Hirobe et al. [26], the electron withdrawing group at the C3 position significantly improved the stability of the TAP core. In addition, the 2,3- bis(methoxycarbonyl)-

TAP exhibited a quantum yield of fluorescence of 15%, which was much higher than 3-(methoxycarbonyl)-TAPs and 3-(4-toluoyl)-TAPs (lower than 1%).

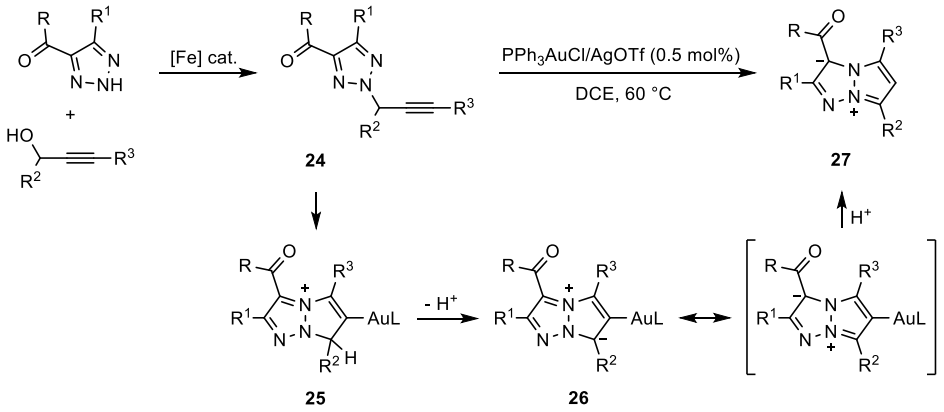

Scheme 7. Gold-mediated synthesis of TAPs **27**.

2.4. Triazolization-Mediated Synthesis

In 2016, our group reported the synthesis of 3-arylated triazapentalene derivatives by using the multicomponent triazolization reaction followed by cyclization as shown in Scheme 8 [32]. Starting from 3-aminopropane-1,2-diol **28**, acetophenones **29**, and *p*-nitrophenyl azide [35], the intermediate 1,2,3-triazoles **30** were prepared. Then, the 3-(triazol-1-yl)propane-1,2-diols **30** underwent sequential substitution and elimination by treatment with triflic anhydride in the basic environment (pyridine/dichloromethane) to afford 3-substituted TAPs **31**.

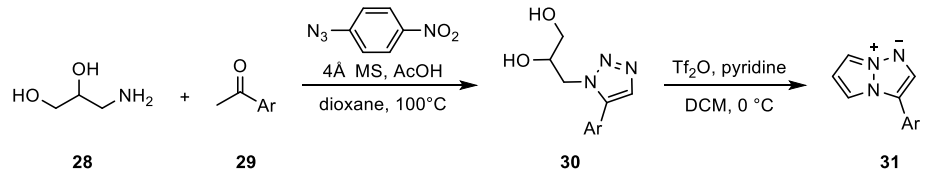

Scheme 8. The synthesis of 3-substituted TAPs **31**.

Compared to previous methods, this two-step pathway started from commercially available compounds and there was no need for toxic transition metal catalysts. However, only TAPs with electron poor aryl groups at the C3 position were successfully obtained.

The fluorescence properties of 3-substituted TAPs were studied in acetonitrile, DCM and toluene [32]. Surprisingly, compound **31a** with a 4-nitrophenyl group at the C3 position showed no fluorescence, which was different from its fluorescent isomer 2-(4-nitrophenyl)-triazapentalene **12g**. In contrast with the other 3-aryl-TAPs **31**, compound **31a** exhibited a longer absorption maximum wavelength and a broader absorption peak (Table 7). These properties of **31a** might be due to the intramolecular charge transfer caused by the nitro group. Compared to the 2-cyanophenyl TAP **12f,** the Stokes shift of compound **31b** (63 nm) was relatively small in DCM, but the quantum yield of fluorescence was quite high (57%). The Stokes shifts of compounds **31b** and **31c** increased as the polarity of the solvent increased, and the full widths at half maximum of emission of compounds **31b** and **31c** were similar to each other. Remarkably, the quantum yield of the fluorescence of compound **31c** was 79% in DCM, which was the highest quantum yield measured so far for any TAP derivative, although this was a lot less in the polar solvent acetonitrile (4%).

Table 7. Fluorescent properties and reaction yields of 3-substituted TAPs **31** in DCM.

	R^3		
			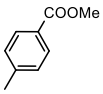
Compound	**31a**	**31b**	**31c**
Yield (%)	69	76	70
$\lambda_{abs,max}$ (nm)	475	401	399
$\lambda_{em,max}$ (nm)	-[a]	464	476
Stokes shift (nm)	-[a]	63	77
$fwhm_{em}$ (cm^{-1})	-[a]	3495	3575
φ_F (%)	-[a]	57	79

[a] No data available.

3. Post-Modifications

3.1. Acetylation and Nitrosation

Although 2-substituted TAPs **5** and **8** were sensitive to air, acetylation and nitrosation of these compounds could be carried out. The TAPs reacted at the C3 position, resulting in 3-acetyl and 3-nitroso derivatives in high yields (Scheme 9) [26]. The successful electrophilic substitution reactions clearly demonstrated the electron rich nature of the TAP core.

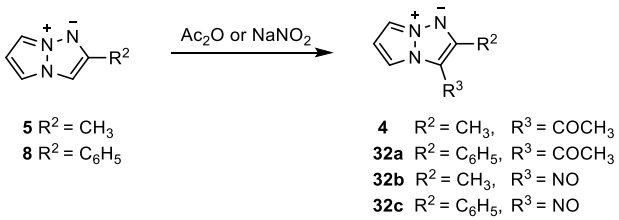

Scheme 9. The acetylation and nitrosation.

3.2. Linearly Bonded 1,3a,6a-Triazapentalene Dimers and Trimer

Starting from the azidotriflate **33** with protected alkyne function, a 2,5-disubstituted TAP with *tert*-butyldimethylsilyl ether (TBS) protecting group was synthesized via click reaction followed by cyclization. The azidotriflate **33** was prepared via a multistep synthesis [36]. After removing the TBS group, the monoethyl-substituted triazapentalene **34** was applied as the starting material together with one more equivalent of **33** in a reiteration of this TAP formation, to develop the linearly bonded oligomeric systems **35** (Scheme 10) [36]. The TAP dimers (n = 2) with different substituents at the C2 position were reported by the Namba group, including a 2-unsubstituted TAP dimer. Unfortunately, the TAP trimers (n = 3) were, in general, too difficult to obtain due to decomposition during the elimination reactions (Table 8). An exception was the derivative with a tridecyl group at the C2 position.

The properties of TAP monomers, TAP dimers, and the TAP trimer were rather similar in the diluted solution in DCM, showing that introducing additional TAP rings had no drastic effect on the fluorescence characteristics [36]. Interestingly, the linearly bonded TAP dimer **35** (n = 2, R = Ph) showed different fluorescence properties when varying the concentration, which suggested changes in the aggregation state. The phenyl-TAP-dimer showed mechanochromic fluorescence in the solid phase and a fluorescence wavelength redshift while going from the crystalline to the amorphous state upon grinding. Emission lifetimes were determined for the solid dimer **35** (n = 2, R = Ph) at 540 nm before ($\lambda_{em,max}$ = 535 nm) and after grinding ($\lambda_{em,max}$ = 590 nm), and were found to be 4.9 and 1.2, respectively. Notably, density functional theory (DFT) calculations verified the planar form of trimer-TAP (R = $C_{13}H_{27}$).

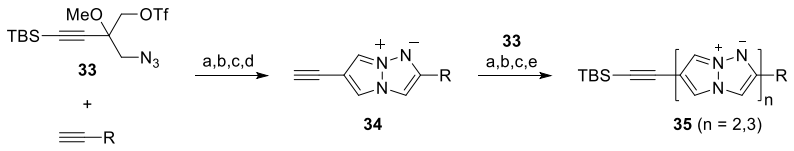

Scheme 10. Synthesis of TAP dimers (n = 2) and trimer (n = 3). (**a**) CuI (5 mol%), BDMAEE (5 mol%), TEA, THF; (**b**) THF, reflux or 50 °C; (**c**) KHMDS, −78 °C; (**d**) TBAF, THF, 0 °C; (**e**) $LiNEt_2$, −78 °C (pyrrolidine lithium salt used for the synthesis of the TAP trimer).

Table 8. Structures and reaction yields of linearly bonded TAPs **35**.

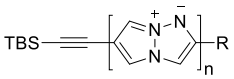	R, Yield (%)				
	$C_{13}H_{27}$				**TBS**
n = 1	52	53	64	59	69
n = 2	75	31	59	17	38
n = 3	42	-[a]	-[a]	-[a]	-[b]

[a] Unsuccessful synthesis from dimer TAP. [b] Decomposed during purification.

3.3. Azo-Coupling Reaction of 3-aryl-1,3a,6a-Triazapentalene

Starting from TAP **31c**, the reaction with benzenediazonium tetrafluoroborate was studied by our group in an attempt to introduce a phenyl group after radical coupling (Scheme 11) [37]. Surprisingly, azo-coupling was observed instead of CH-arylation, which was most probably due to the marked nucleophilic character of the triazapentalene. It was intriguing that under the reaction circumstances, a rearranged 2-aryl-TAP **37** was readily formed and isolated as the major product, accompanied by an azo-coupled 3-aryl-TAP **36** as the minor product. The molecular structures of the products were elucidated using single-crystal X-ray diffraction analysis. A mechanism towards TAP **37** involving the formation of an open chain nitrilimine and alternative ring closure was proposed. Different attempts were carried out to reduce azo compound **37**, which led to cleavage of the TAP core rather than the formation of the amino derivative.

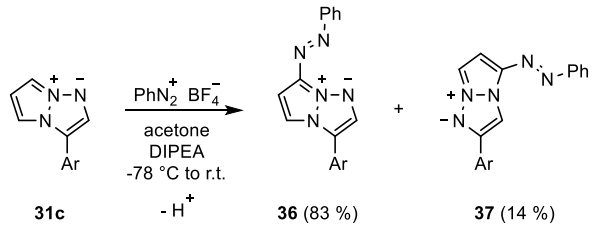

Scheme 11. Azo coupling of 3-aryl-TAP **31c** towards 6-azo derivative **36** and rearranged 4-phenylazo-2-aryl-TAP **37**. Ar = 4-MeOCO-C_6H_4.

4. Applications

The fluorescent TAP core has been studied by the Namba group as an element of biological imaging probes and sensors. All TAP products discussed within this section were synthesized via the CuAAC-based strategy.

The first application concerns the use of TAP as a fluorescent probe for live cell imaging [28]. Compound **12i** was selected as the fluorescent dye due to its small but significant solubility in water and because it combines a long fluorescent wavelength with acceptable stability under UV irradiation (Scheme 12). After treatment with a DMSO solution of the fluorescent dye **12i**, staining of Hela cells was clearly observed with fluorescence microscopy and no cytotoxic effect was seen during the observation period.

Then, the TAP **12i** was developed as a fluorescent reagent to label glycine ethyl ester and tripeptide Gly-Pro-Leu [28]. By treating methyl ester TAP **12i** with lithium hydroxide, a benzoic acid derivative was obtained that was directly converted into an activated *N*-hydroxysuccinimide (NHS) ester **38**. As the purification from the DCC-derived urea was troublesome, instead, polymer-supported DCC was used and could be filtered off to give pure reactive ester **38**. Subsequently, compound **38** was reacted with glycine ethyl ester and tripeptide Gly-Pro-Leu to obtain the labeled glycine **39** and tripeptide **40**, respectively. Compounds **39** and **40** showed the same fluorescence maximum at 567 nm with 37% and 24% fluorescence quantum yields in DCM, respectively. The fluorescence measurements for these compounds in water demonstrated decreased Stokes shifts and quantum yields.

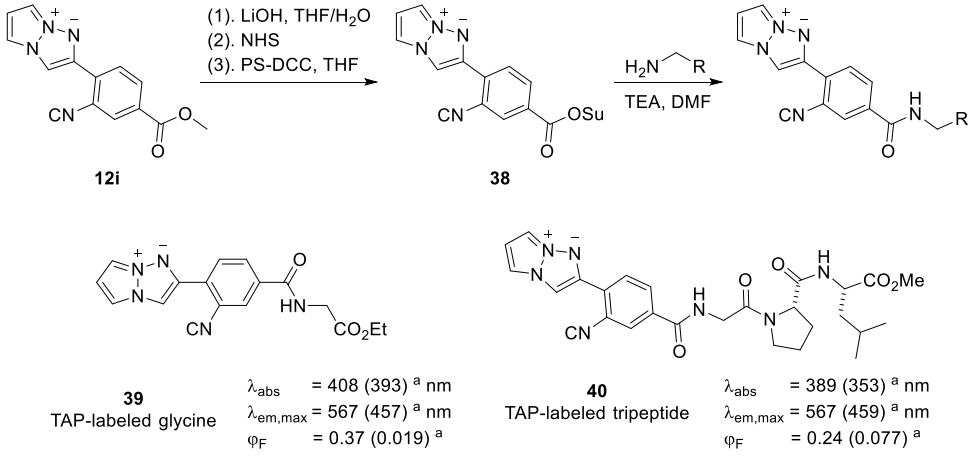

Scheme 12. Synthesis of TAP-labeled labeled glycine **39** and tripeptide **40** and properties in DCM. [a] Measured in water. Su = succinimide.

The second application was based on compound **12e** (Figure 2), which showed high fluorescence intensity in phosphate-buffered saline (PBS) and was applied as a fluorescent probe to observe cellular differentiation processes in various living cells [38]. After treatment with a PBS solution of **12e**, cytoplasmic and nuclear morphological changes during the differentiation processes were monitored by fluorescence microscopy. It was found that the fluorescence probe **12e** had no toxicity, neither was there an effect on the cellular differentiation processes, and the probe could be easily washed away from the cells that can continue to culture for following studies.

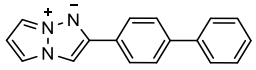

Figure 2. The 2-([1,1′-Biphenyl]-4-yl)-TAP **12e**.

In a third application, TAP analogs of biphenyl-type kinesin spindle protein (KSP) inhibitors **41** and **42** (Figure 3) were prepared and investigated as bifunctional fluorescent probes [39]. Both analogs showed inhibitory activity against KSP ATPase, although **42** was more potent (half maximal inhibitory concentration (IC_{50}) was 6.8 μM). Further microscopic studies were carried out with **42** in cultured cells in order to visualize the intracellular distribution. The partial colocalization of compound **42** with KSP, combined with its inhibitory activity, demonstrated the potency of the TAP fluorophore to be used as a probe for the visualization of bioactive substances and their targets.

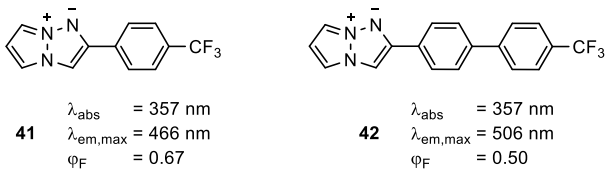

Figure 3. Structure and properties of 2-(4-(trifluoromethyl)phenyl)-TAP **41** and 2-(4′-(trifluoromethyl)-[1,1′-biphenyl]-4-yl)-TAP **42** in DCM.

Most recently, a compact vinyl ketone functionalized TAP **45** was cleverly designed by Namba et al. as a thiol-specific fluorescent labeling reagent [40]. Starting from the previously reported 2-methoxycarbonyl-TAP **43**, the electrophilic α,β-unsaturated ketone TAP **45** was prepared via a high-yielding multistep synthesis involving Weinreb amide **44** (Scheme 13). The 2-vinyl ketone-TAP **45** was then reacted with various thiols via thiol Michael additions to obtain compounds **46**. Remarkably, the fluorescence intensity of **45** was turned off due to the conjugation of the vinyl ketone at the C2 position. After the addition of the thiol group, this conjugation was interrupted, and the fluorescence of compound **46** was turned on again while also exhibiting shorter emission wavelengths as compared to **45**. A water-soluble R8 peptide was also successfully labeled in a phosphate buffer (pH 7). Although no fluorescence was observed in water, the labeled peptide became luminescent after uptake and localization in the hydrophobic regions of A549 cells. Advantageously, the vinyl ketone TAP did not cause any background fluorescence and was not found to be cytotoxic. Next, a captopril-TAP conjugate was prepared for drug imaging. Captopril is a cysteine derivative that inhibits angiotensin converting enzyme (ACE) and has been used for the treatment of hypertensive patients. The inhibitory activity and confocal laser microscope imaging studies in vascular endothelial cells demonstrated that the fluorophore had no impact on the activity of captopril and that the fluorophore could be used as a probe for mechanistic studies.

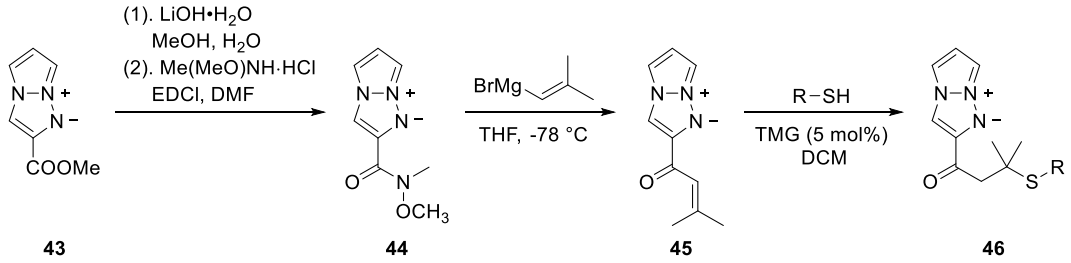

Scheme 13. The synthesis of TAP labeling reagent **45** and thiol adducts **46**.

In a final application, TAP derivative **51** was used as a fluorescent sensor for iron (Scheme 14) [41]. Starting with a protected catechol-containing alkyne **48** and azide **10a**, TAP **49** was obtained via the CuAAC reaction strategy. In order to increase the stability, an acetyl group was introduced into compound **49** at the C3 position through acylation. The acetylated compound **50** was further conjugated to serine trimer **47** by saponification and amide coupling. After deprotection with HCl, the TAP labeled enterobactin **51** was obtained. The influence of iron on the fluorescent properties of sensor **51** was studied with $Fe(acac)_3$ as an Fe^{3+} ion source at different concentrations. When increasing the amount of Fe^{3+} in a DMSO solution of **51**, the fluorescence intensity was decreased gradually, with complete disappearance at 1.2 equivalents of $Fe(acac)_3$. The emission maximum did not change. In DMF and *tert*-butanol, a similar phenomenon was observed. Fourth-period metals also caused a clear decrease in fluorescence intensity, although no complete quenching was observed, even while adding 5.0 equivalents. Thus, 1,3a,6a-triazapentalene-labeled enterobactin **51** was shown to be a selective and highly sensitive fluorescence-quenching sensor for iron (III).

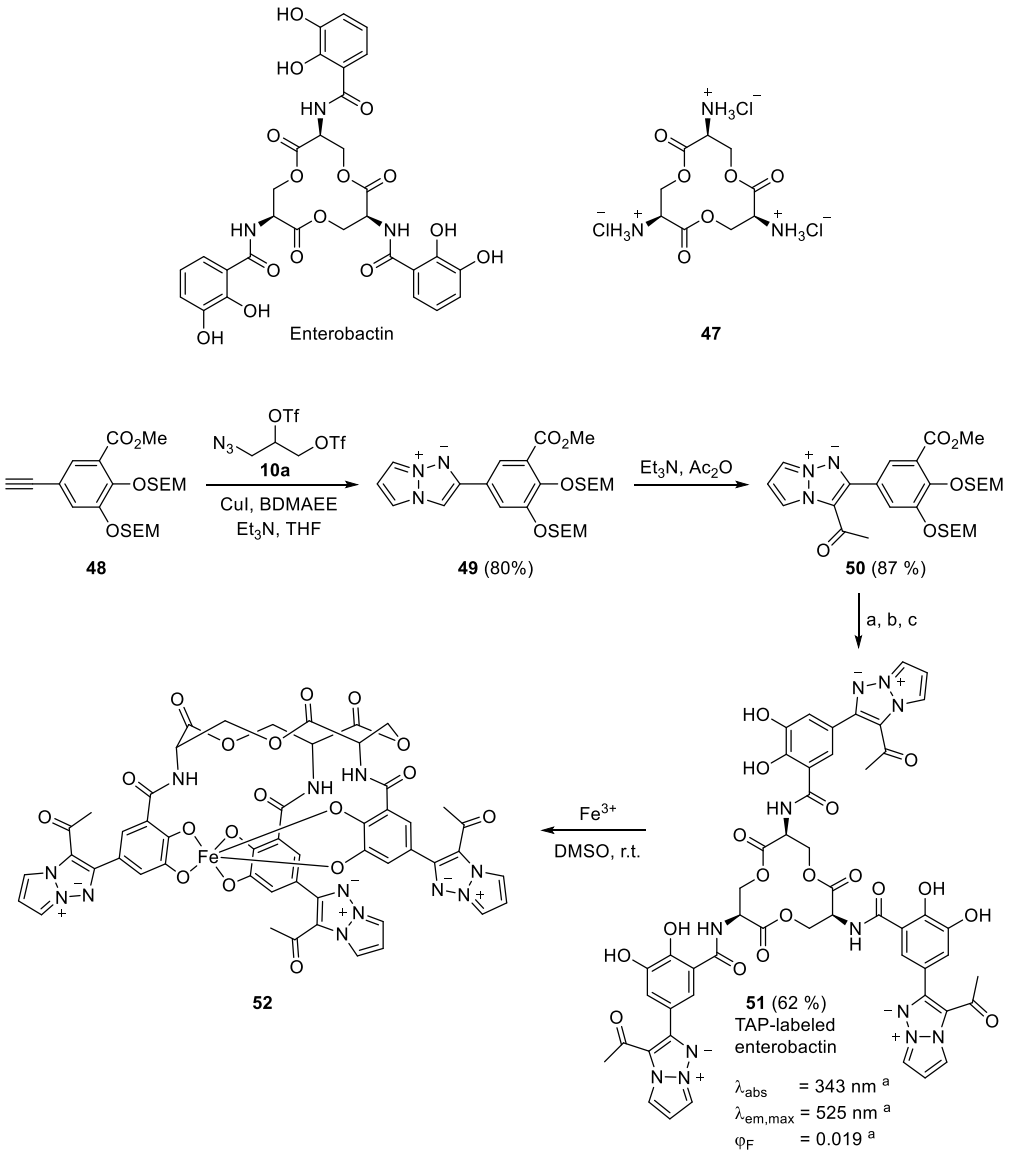

Scheme 14. Synthesis of fluorescence quenching sensor **51**. (**a**) LiOH·H_2O, dioxane/H_2O, 55 °C; (**b**) **47** (1.0 equivalent), DMTMM, DIPEA, MeOH; (**c**) 0.5 M HCl, *i*PrOH. [a] Measured in DMSO.

5. Conclusions

In this mini review, we have discussed the different synthetic methodologies of bicyclic 1,3a,6a-triazapentalenes. An alternative to the earlier synthesis from pyrazoles and aminating reagents was provided by the CuAAC-based strategy, which could be used to synthesize a wide scope of 2-substituted TAPs. The gold-catalyzed cyclization pathway afforded excellent yields of highly functionalized TAPs with electron withdrawing functional groups at the C3 position. Unfortunately, the starting materials for these methods often need to be prepared via a multistep synthesis. The triazolization-mediated synthesis provided access to 2-unsubstituted TAPs from readily available starting materials. Therefore, this was complementary to the previous strategies.

As a result of the profound studies by Namba et al., the substituent effects on the properties of TAP are known and could allow one to design the fluorophores according to the requirements of a particular application. For example, the stability of the TAP core could at first be ensured by introducing an electron withdrawing group at the C3 position, while the fluorescence wavelength could be adjusted by variation of the substituent at the C2 position. Further adjustments of the properties could be made with the substituent at the C4,

C5 or C6 position. For instance, the extinction coefficient and therefore brightness of TAPs could be increased by introducing a substituent at the C4 position. For the TAP compounds that require high quantum yields, often it is a good idea to introduce a substituent at the C5 or C6 position.

Applications of TAPs were mainly focused on live-cell fluorescence imaging, in particular drug imaging, although an application as iron chemosensor was also reported. The small size of the TAP core is often mentioned as an advantage compared to other fluorescent probes. Up to this moment, reports about TAP probes and sensors have been limited to 2-substituted TAPs, which are obtained via the CuAAC method. Problems that often occur and still need to be solved are poor solubility and weak fluorescence intensity of the TAP probes in water.

We are only at the start of the applications of this new and compact fluorophore TAP. Hopefully, this review will stimulate further investigations.

Funding: This research received no external funding.

Institutional Review Board Statement: Not applicable.

Informed Consent Statement: Not applicable.

Data Availability Statement: Data sharing not applicable.

Acknowledgments: Yingchun Wang acknowledges the China Scholarship Council for a doctoral fellowship (201706920044); Tomas Opsomer thanks the FWO-Vlaanderen for a doctoral fellowship (1154419N) and KU Leuven for a postdoctoral mandate (PDM/20/091). Wim Dehaen acknowledges financial support from KU Leuven (Project C14/19/78).

Conflicts of Interest: The authors declare no conflict of interest.

References

1. Rezende, L.; Emery, F. A review of the synthetic strategies for the development of BODIPY dyes for conjugation with proteins. *Orbital: Electron. J. Chem.* **2013**, *5*, 62–83.
2. Sameiro, M.; Gonçalves, T. Fluorescent labeling of biomolecules with organic probes. *Chem. Rev.* **2009**, *109*, 190–212. [CrossRef]
3. Wu, D.; Chen, L.; Lee, W.; Ko, G.; Yin, J.; Yoon, J. Recent progress in the development of organic dye based near-infrared fluorescence probes for metal ions. *Coord. Chem. Rev.* **2018**, *354*, 74–97. [CrossRef]
4. Jiao, X.; Li, Y.; Niu, J.; Xie, X.; Wang, X.; Tang, B. Small-Molecule Fluorescent Probes for Imaging and Detection of Reactive Oxygen, Nitrogen, and Sulfur Species in Biological Systems. *Anal. Chem.* **2018**, *90*, 533–555. [CrossRef] [PubMed]
5. Wang, L.; Frei, M.S.; Salim, A.; Johnsson, K. Small-Molecule Fluorescent Probes for Live-Cell Super-Resolution Microscopy. *J. Am. Chem. Soc.* **2019**, *141*, 2770–2781. [CrossRef] [PubMed]
6. Terai, T.; Nagano, T. Small-molecule fluorophores and fluorescent probes for bioimaging. *Pflügers Arch.* **2013**, *465*, 347–359. [CrossRef]
7. Benniston, A.C.; Copley, G. Lighting the way ahead with boron dipyrromethene (Bodipy) dyes. *Phys. Chem. Chem. Phys.* **2009**, *11*, 4124–4131. [CrossRef]
8. Fu, Y.; Finney, N.S. Small-molecule fluorescent probes and their design. *RSC Adv.* **2018**, *8*, 29051–29061. [CrossRef]
9. Formica, M.; Fusi, V.; Giorgi, L.; Micheloni, M. New fluorescent chemosensors for metal ions in solution. *Coord. Chem. Rev.* **2012**, *256*, 170–192. [CrossRef]
10. Cho, D.G.; Sessler, J.L. Modern reaction-based indicator systems. *Chem. Soc. Rev.* **2009**, *38*, 1647–1662. [CrossRef]
11. Boens, N.; Leen, V.; Dehaen, W. Fluorescent indicators based on BODIPY. *Chem. Soc. Rev.* **2012**, *41*, 1130–1172. [CrossRef] [PubMed]
12. Yu, C.; Fang, X.; Wu, Q.; Jiao, L.; Sun, L.; Li, Z.; So, P.K.; Wong, W.Y.; Hao, E. A Family of BODIPY-like Highly Fluorescent and Unsymmetrical Bis(BF_2) Pyrrolyl–Acylhydrazone Chromophores: BOAPY. *Org. Lett.* **2020**, *22*, 4588–4592. [CrossRef] [PubMed]
13. Pookkandam Parambil, S.; de Jong, F.; Veys, K.; Huang, J.; Veettil, S.P.; Verhaeghe, D.; Van Meervelt, L.; Escudero, D.; Van der Auweraer, M.; Dehaen, W. BOPAHY: A doubly chelated highly fluorescent pyrrole–acyl hydrazone–BF_2 chromophore. *Chem. Commun.* **2020**, *56*, 5791–5794. [CrossRef] [PubMed]
14. Boens, N.; Verbelen, B.; Dehaen, W. Postfunctionalization of the BODIPY Core: Synthesis and Spectroscopy. *Eur. J. Org. Chem.* **2015**, *2015*, 6577–6595. [CrossRef]
15. Huaulmé, Q.; Mirloup, A.; Retailleau, P.; Ziessel, R. Synthesis of highly functionalized BOPHY chromophores displaying large stokes shifts. *Org. Lett.* **2015**, *17*, 2246–2249. [CrossRef]
16. Loudet, A.; Burgess, K. BODIPY dyes and their derivatives: Syntheses and spectroscopic properties. *Chem. Rev.* **2007**, *107*, 4891–4932. [CrossRef]

17. Namba, K.; Osawa, A.; Ishizaka, S.; Kitamura, N.; Tanino, K. Direct synthesis of fluorescent 1,3a,6a-triazapentalene derivatives via click-cyclization-aromatization cascade reaction. *J. Am. Chem. Soc.* **2011**, *133*, 11466–11469. [CrossRef]
18. Nyffenegger, C.; Pasquinet, E.; Suzenet, F.; Poullain, D.; Jarry, C.; Léger, J.; Guillaumet, G. An efficient route to polynitrogen-fused tricycles via a nitrene-mediated N-N bond formation under microwave irradiation. *Tetrahedron* **2008**, *64*, 9567–9573. [CrossRef]
19. Lynch, B.M.; Hung, Y.Y. Pyrazolo[1,2-*a*]benzotriazole and related compounds. *J. Heterocycl. Chem.* **1965**, *2*, 218–219. [CrossRef]
20. Tsuge, O.; Samura, H. Studies of polyazapentalenes. II. The preparation of 1,3a,6a-triazapentalenes. *Org. Prep. Proced. Int.* **1972**, *4*, 273–281. [CrossRef]
21. Nyffenegger, C.; Pasquinet, E.; Suzenet, F.; Poullain, D.; Guillaumet, G. Synthesis of nitro-functionalized polynitrogen tricycles bearing a central 1,2,3-triazolium ylide. *Synlett* **2009**, *3*, 1318–1320. [CrossRef]
22. Sirbu, D.; Diharce, J.; Martinić, I.; Chopin, N.; Eliseeva, S.V.; Guillaumet, G.; Petoud, S.; Bonnet, P.; Suzenet, F. An original class of small sized molecules as versatile fluorescent probes for cellular imaging. *Chem. Commun.* **2019**, *55*, 7776–7779. [CrossRef] [PubMed]
23. Kim, T.; Kim, K.; Park, Y.J. A Novel Method for the Synthesis of 2,3-Benzo-1,3a,6a-triazapentalenes through Pummerer-Type Reactions of γ-(Benzotriazol-1-yl) allylic Sulfoxides. *Eur. J. Org. Chem.* **2002**, 493–502. [CrossRef]
24. Katritzky, A.R.; Hür, D.; Kirichenko, K.; Ji, Y.; Steel, P.J. Synthesis of 2,4-disubstituted furans and 4,6-diaryl-substituted 2,3-benzo-1,3a,6a-triazapentalenes. *Arkivoc* **2004**, *2004*, 109–121. [CrossRef]
25. Daniel, M.; Hiebel, M.A.; Guillaumet, G.; Pasquinet, E.; Suzenet, F. Intramolecular Metal-Free N−N Bond Formation with Heteroaromatic Amines: Mild Access to Fused-Triazapentalene Derivatives. *Chem. Eur. J.* **2020**, *26*, 1525–1529. [CrossRef]
26. Koga, H.; Hirobe, M.; Okamoto, T. Mesoionic 1,3a,6a-triazapentalenes. *Tetrahedron Lett.* **1978**, 1291–1294. [CrossRef]
27. Namba, K.; Mera, A.; Osawa, A.; Sakuda, E.; Kitamura, N.; Tanino, K. One-Pot Synthesis of Highly Fluorescent 2,5-Disubstituted-1,3a,6a-triazapentalene. *Org. Lett.* **2012**, *14*, 5554–5557. [CrossRef]
28. Namba, K.; Osawa, A.; Nakayama, A.; Mera, A.; Tano, F.; Chuman, Y.; Sakuda, E.; Taketsugu, T.; Sakaguchi, K.; Kitamura, N.; et al. Synthesis of yellow and red fluorescent 1,3a,6a-triazapentalenes and the theoretical investigation of their optical properties. *Chem. Sci.* **2015**, *6*, 1083–1093. [CrossRef]
29. Nakayama, A.; Nishio, S.; Otani, A.; Mera, A.; Osawa, A.; Tanino, K.; Namba, K. Substituent effect at the C4-position of 1,3a,6a-triazapentalene. *Chem. Pharm. Bull.* **2016**, *64*, 830–837. [CrossRef]
30. Mera, A.; Ito, M.; Nakayama, A.; Namba, K. Synthesis of 2,6-Disubstituted-1,3a,6a-Triazapentalenes and Their Fluorescence Properties. *Chem. Lett.* **2017**, *46*, 539–542. [CrossRef]
31. Cai, R.; Wang, D.; Chen, Y.; Yan, W.; Geise, N.R.; Sharma, S.; Li, H.; Petersen, J.L.; Li, M.; Shi, X. Facile synthesis of fluorescent active triazapentalenes through gold-catalyzed triazole-alkyne cyclization. *Chem. Commun.* **2014**, *50*, 7303–7305. [CrossRef] [PubMed]
32. Verbelen, B.; Dehaen, W. Two-Step Synthesis of Fluorescent 3-Arylated 1,3a,6a-Triazapentalenes via a Three-Component Triazolization Reaction. *Org. Lett.* **2016**, *18*, 6412–6415. [CrossRef] [PubMed]
33. Osawa, A.; Mera, A.; Namba, K.; Tanino, K. Transformations of 1-(oxiranylmethyl)-1,2,3-triazoles into 2-(Oxiranylmethyl)-1,2,3-triazoles and alkanenitriles. *Synlett* **2013**, *24*, 207–210. [CrossRef]
34. Yan, W.; Wang, Q.; Chen, Y.; Petersen, J.L.; Shi, X. Iron-catalyzed C-O bond activation for the synthesis of propargyl-1,2,3-triazoles and 1,1-bis-triazoles. *Org. Lett.* **2010**, *12*, 3308–3311. [CrossRef]
35. Opsomer, T.; Van Hoof, M.; D'Angelo, A.; Dehaen, W. 1,2,3-Triazole-Mediated Synthesis of 1-Methyleneisoquinolines: A Three-Step Synthesis of Papaverine and Analogues. *Org. Lett.* **2020**, *22*, 3596–3600. [CrossRef]
36. Ito, M.; Mera, A.; Mashimo, T.; Seki, T.; Karanjit, S.; Ohashi, E.; Nakayama, A.; Kitamura, K.; Hamura, T.; Ito, H.; et al. Synthesis and Evaluation of a 1,3a,6a-Triazapentalene (TAP)-Bonded System. *Chem. A Eur. J.* **2018**, *24*, 17727–17733. [CrossRef]
37. Wang, Y.; Opsomer, T.; Van Meervelt, L.; Dehaen, W. Ring-degenerate rearrangement resulting from the azo coupling reaction of a 3-aryl-1,3a,6a-triazapentalene. *J. Org. Chem.* **2020**, 1–6. [CrossRef]
38. Kamada, R.; Tano, F.; Kudoh, F.; Kimura, N.; Chuman, Y.; Osawa, A.; Namba, K.; Tanino, K.; Sakaguchi, K. Effective cellular morphology analysis for differentiation processes by a fluorescent 1,3a,6a-Triazapentalene derivative probe in live cells. *PLoS ONE* **2016**, *11*, e0160625. [CrossRef]
39. Sawada, J.; Osawa, A.; Takeuchi, T.; Kaneda, M.; Oishi, S.; Fujii, N.; Asai, A.; Tanino, K.; Namba, K. Functional 1,3a,6a-triazapentalene scaffold: Design of fluorescent probes for kinesin spindle protein (KSP). *Bioorg. Med. Chem. Lett.* **2016**, *26*, 5765–5769. [CrossRef]
40. Nakayama, A.; Otani, A.; Inokuma, T.; Tsuji, D.; Mukaiyama, H.; Nakayama, A.; Itoh, K.; Otaka, A.; Tanino, K.; Namba, K. Development of a 1,3a,6a-triazapentalene derivative as a compact and thiol-specific fluorescent labeling reagent. *Commun. Chem.* **2020**, *3*, 6. [CrossRef]
41. Hayashi, T.; Osawa, A.; Watanabe, T.; Murata, Y.; Nakayama, A.; Namba, K. Development of 1,3a,6a-triazapentalene-labeled enterobactin as a fluorescence quenching sensor of iron ion. *Tetrahedron Lett.* **2017**, *58*, 1961–1964. [CrossRef]